JOURNAL OF OPTOELECTRONICS AND ADVANCED MATERIALS, Vol. 10, No. 11, November 2008, p. 2819 - 2826

*Review Paper*

# Spectroscopic characterization of nanocrystalline diamond

N. WOEHRL*, V. BUCK
*Division of Thin Film Technology, Department of Physics, University of Duisburg-Essen, 47048 Duisburg, Germany*

Diamond films are of interest for many tribological applications because of the outstanding combination of favourable properties like highest hardness, low coefficient of friction, high wear resistance, high thermal conductivity, and chemical inertness. The development of low pressure synthesis for diamond films on nondiamond substrates was responsible for the rapid growth of diamond coating technology for several applications and many different chemical vapour deposition (CVD) processes for the production of thin diamond films have been developed; especially the development of nanocrystalline diamond films that are aditionally tough and smooth opened a new area. But it has been proven difficult to coat technically important substrates like ceramics, steels, nickel alloys, cemented carbides, and most alloys containing transition metals with well-adherent, high quality diamond films. However, diamond coatings with good adhesion and wear resistance are necessary to realize the full potential of cutting tools or abrasive applications and to get a good performance in machining of advanced materials. Apart from several other aspects, problems due to the difference in thermal expansion coefficients of diamond and the substrate and intrinsic mechanical stresses due to the growth process of diamond films have to be solved. It is shown here how these problems can be solved by careful adjustment of the process parameters determining film structure and thus mechanical stress; especially it is shown that mechanical stress can be determined quantitavely by non destructive spectroscopic methods that allow quality assurance even on substrates with complicated shape ("3D-substrates") like tools.

(Received September 1, 2008; accepted October 30, 2008)

*Keywords*: Nanocrystalline diamond films, Residual stress

## 1. Introduction

For many years carbon films are now established in thin film technology. Because carbon atoms can be $sp^3$, $sp^2$- and sp bonded, there are different forms of carbon films (e.g. graphite, diamond, fullerens, carbon nanotubes and DLC) giving a broad possibility for nanostructuring of the material by alternating different structures in nanometer size. In doing so one can classify nanostructured materials based on the dimension of the structuring in zero-, one- and three-dimensional respectively, depending on whether one uses cluster in a matrix (zero-dimensional), filaments in a matrix (one-dimensional), Sandwiches of thin films (two-dimensional) or nanometer sized crystals (three-dimensional).

Adding of additional elements such as hydrogen extends the potentional applications even further – the term DLC coined for amorphous carbon films (from "Diamond Like Carbon, DLC") alone describes a whole class of materials and includes different materials that can for example consist entirely of carbon (a-C), of carbon and hydrogen in different concentrations (a-C:H), or different constituents like metals (Me-C:H) or silicon, oxygen, halogens or nitrogen.

All these materials have some properties in common such as the biocompatibility and chemical inertness – other properties can be adjusted in a wide range such as hardness (from soft to extreme hard), electric conductivity (insulating to conductive), wettability (from hydrophobic to hydrophilic) or elasticity (more than one order of magnitude) and found numerous applications e.g. as tribological coatings, as barrier coatings or as a coating for medical implants such as stents or artificial hip joints.

From the viewpoint of nanotechnology a straightforeward extension of thes homogeneous amorphous films establishing more and more in recent years are the nanocrystalline diamond films (NCD[1]) consisting of nanometer sized diamond grains embedded in the amorphous matrix.

One particularly important film property to be controlled is the residual stress. High residual stresses in thin films lead to reduced adhesion, that can at one point even lead to delamination of the film from the substrate. In other cases the residual stress leads to cracks in the films limiting their functional capability. Fig. 1 shows these two effects of residual stress in thin films. Fig. 1a shows a DLC film that was delaminating because of high compressive stress, Fig 1b shows a NCD film with cracks due to high tensile stress.

But also less dramatic effects make the investigation and control of the residual stress an interesting field. For instance physical properties (optical, electrical, and magnetic) can be influenced by residual stress in the films.

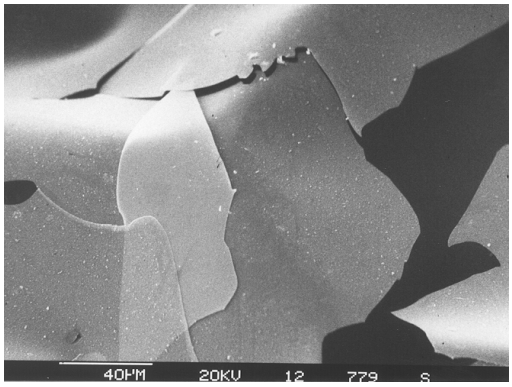


*a)*

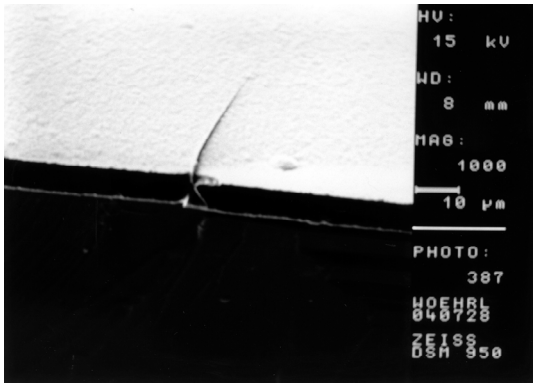


*b)*

*Fig. 1 Residual stress in thin films.*

## 2. Origin of residual stress in thin films

First works investigating the residual stress in thin films were done by Stoney [2] at the beginning of the last century. Depositing metal films on substrates by electrolysis he observed, that the films started to develop cracks and peel of the substrate when exceeding a specific film thickness. By systematic investigations he not only found out that the residual stress is scaling with the film thickness but he also found a way to measure the stress. With respect to Stoney's equation it was possible to quantitatively determine the residual stress from the stress induced curvature of the substrate. Up to now his method, based on the measurement of the bending of the substrate, is used in various methods to measure the residual stress in thin films.

It should be noted here that spectral methods of determining stress for example from the shift of Raman peaks or the shift and broadening of lines obtained by x-ray defraction measurements can measure the stress in the crystalline grains but not the contribution from the grain boundaries thus making these methods valuable to obtain additional information about the stress in the films but not necessarily to obtain the overall stress in the films. Furthermore the possible application of these spectral methods is of course limited when used for nanostructured materials, because the small crystals in films lead to a broadening of the spectral lines and therefore limit the accuracy of the methods.

Mechanical stress in thin films arises from different effects, that are due to the properties of the materials used on the one hand and due to the process parameters of the deposition itself on the other hand.

The residual stress in thin films is the sum of two components – the thermal stress $\sigma_{th}$ and the intrinsic stress $\sigma_{in}$ (if epitaxial growth and lattice mismatch effects can be excluded).

$$\sigma = \sigma_{th} + \sigma_{in} \tag{1}$$

The thermal stress $\sigma_{th}$ arises from the difference of thermal expansion coefficients of substrate and film material because of the elevated temperature during the deposition. After the deposition the substrate is cooled down to the ambient temperature and both the substrate and the film contract according to their thermal expansion coefficients. When the two materials have different thermal expansion coefficients they contract differently resulting in residual stress in the film just as known from bimetals. This stress component can be calculated [3, 4] by

$$\sigma_{th} = E_f(\alpha_f - \alpha_S)(T_B - T_M) \tag{2}$$

In this equation $E_f$ represents the elastic modulus of the deposited film, $\alpha_f$ and $\alpha_S$ the mean values for the thermal expansion coefficient of the film and the substrate respectively and $T_B$ and $T_M$ the temperature during the deposition and the stress measurement. Thus with known material constants one can calculate the fraction of the thermal stress to the residual stress in the film.

The intrinsic part of the residual stress consists of two independent contributions. The "grain boundaries mismatch model" [5] describes the origin of tensile stress in films: In the early steps of the deposition only isolated nuclei grow on the substrate. At these nuclei the film growth will take place, as long as the isolated growth zones get in contact with each other. At this point it is improbable that the gap between two growth zones is exactly of the size of one atom. More probable is a gap that is slightly bigger than one atom diameter. Because a closed film surface is energetic more preferable for the film the atoms attract one another to close the gap. This process leads to attractive forces between the atoms that result in tensile stress in the film. Fig. 2 graphically shows this effect and the bending of a substrate that was coated with a film under tensile stress.

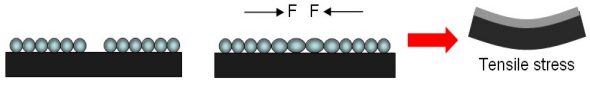


*Fig. 2. Evolution of tensile stress in thin films.*

One can deduce from the "grain boundaries mismatch model" that the arising tensile stress must be proportional to the reciprocal grain size of the film. The tensile stress thus gets bigger the smaller the grain size is. This fact is to be considered, especially when the grain size can be varied by the process parameters and the residual stress be tailored by this. It should be mentioned here that a variation in grain size as a function from the distance to the substrate surface e.g. by selective grain growth (van der Drift) can generate stress gradients in the film.

In contrast to this model the "ion-peening model" describes the origin of compressive stress in films, like it e. g. occurs during sputter deposition of thin films [6].

When high energetic particles bombard the already deposited film surface they do not necessarily condensate on the surface, but penetrate, depending on their energy, into the film. In doing so the already deposited film gets densified and compressed. The resulting compressive stress is therefore strongly depending on the energy of the impinging particles and can easily be adjusted by this parameter. Fig. 3 schematically shows this process and the influence on the curvature of the substrate.

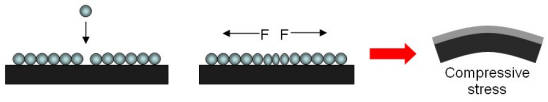


*Fig. 3. Evolution of compressive stress in thin films.*

## 3. Residual stress and Substrate Curvature

Like mentioned before residual stress in thin films leads to a bending of the substrate. This bending can be measured and the residual stress quantitatively derived from it. Ideally long, narrow samples (length:width ratio 2:1) are used for stress measurements so that the Stoney equation can be used to calculate the residual stress:

$$\sigma = \frac{E_{sub}}{(1-\nu)} \frac{t_{sub}^2}{6 \cdot t_{film}} \left( \frac{1}{R_{post}} - \frac{1}{R_{pre}} \right) \qquad (3)$$

It is striking and feasible that primarily only material constants are needed to calculate the residual stress with this equation: $E_{sub}$ represents the elastic modulus of the substrate; ν is the Poisson ratio of the substrate and $t_{sub}$ the substrate thickness. Solely the film thickness $t_{film}$ must be measured as only information of the film. $R_{post}$ and $R_{pre}$ represent the curvature of the sample measured before and after the deposition respectively because for the calculation of the residual stress in the film the change in the curvature of the substrate is essential. The maximum residual stress and the resolution of the stress measurements strongly depend on the boundary conditions of the measurement. As one can get from the Stoney equation substrate material, substrate thickness and film thickness need to be considered. Exemplarily the numbers for a 1µm thick film on a silicon wafer of 425µm thickness shall be given. In this case the maximum of residual stress measurable with our setup is 5.5GPa with a resolution of around 1.4MPa at a substrate curvature of 4km.

The determination of the curvature is equivalent to the fitting of a circle, or, because the length of the substrate is usually much smaller than the curvature, a parabola to the contour of the substrate as shown in Fig. 4.

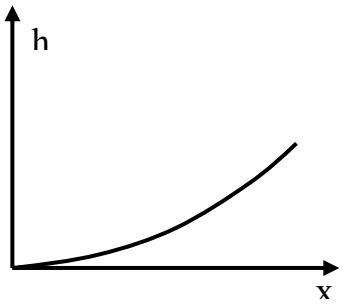


*Fig. 4. Fitting of a circle or a parabola respectively to the contour of the substrate.*

$$h(x) = \frac{1}{R} x^2 + bx + c \qquad (4)$$

It is evident that for the fitting the height must be measured for at least three positions x. If it is not necessary to calculate the centre of the circle two tangents or angles at known positions are sufficient according to

$$h'(x) = \frac{2}{R} x + b \qquad (5)$$

It should be mentioned here that formerly frequently used setups, which were using one sided clamping at x=0 and measuring h only at the loose end lead to errors due to thermal drift.

## 4. Optical measurement systems (Surface Stress Induced Optical Deflection: „SSIOD")

Different methods for the determination of the curvature of a sample are known in the literature [7, 8, 9]. Here, two optical methods are used that allow to get the curvature from electrical signals. Both methods use the fact that a laser beam is deflected in a specific angle depending on the curvature of the sample when scanning across it. The measurement of at least two reflection angles allows calculating the curvature. Fig. 5a shows this principle schematically first for a flat sample. The laser beam stikes the sample perpendicular to the surface and is reflected in the same direction. Striking a curved surface though the laser beam will be reflected according to the law of reflection [Fig. 5b].

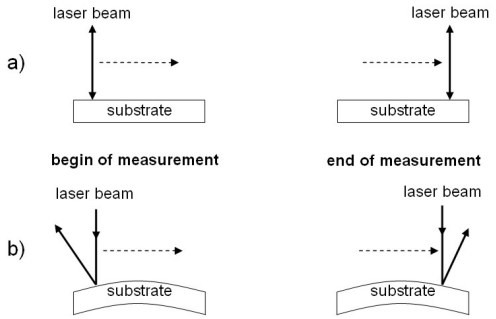


*Fig. 5. Optical principle of SSIOD method.*

The setup for the first apparatus used [10] is shown schematically in Fig. 6. The measurement of the angle of reflection is done by a position sensing diode (PSD). The PSD is in principle a one-dimensional expanded "normal" diode. It consists beside of one ground contact in the middle of the diode of two electrical contacts at each end of the diode over which the laser induced current can drain off. By comparing the two currents and standardization to the overall current one gets the position information of the focused laser beam spot on the diode, independent from the light intensity. All optical components are set up on a vibration absorbing optical bench. The laser beam (3) is reflected by mirrors (4) onto the substrate (5) and reflected back onto the position sensing diode (6). The optical path length of the laser is a decisive factor for the sensitivity of the setup and was therefore extended by the mirrors (current optical path length of 1m). The laser and the PSD are mounted on a linear positioning stage (2) which allows to scan over the sample. Although – like shown earlier – the measuring of two reflection angles would be sufficient, the angles at 60 positions are measured to increase the accuracy of the measurement.

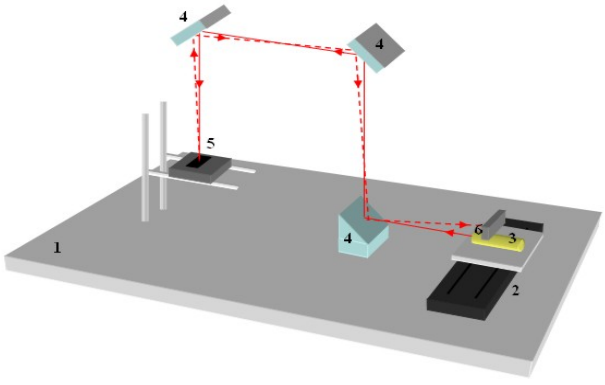


*Fig. 6. Setup to measure strong curved samples 1) vibration absorbing optical bench 2) linear positioning stage 3) laser 4) mirrors 5) substrate on stage 6) Position sensing diode (PSD).*

Fig. 7 shows the measurement of a curved sample. The diagram shows the position the laser spot hits the PSD while scanning over the sample. From the slope of the linear fit of the data points one can calculate the curvature of the sample.

As mentioned before, the sensitivity of the SSIOD method strongly depends on the geometry of the set up, such as the distance between the sample and the detector. In the current configuration the minimal radius that can be measured is $R_{min}$=4m when the whole detector length is used. However much smaller radii can be measured nonetheless.

In this case the reflected angle of the laser beam extends the length of the PSD during the measurement. When the thereby reduced scanned sample length is considered in the evaluation, radii down to one meter and even below can be measured.

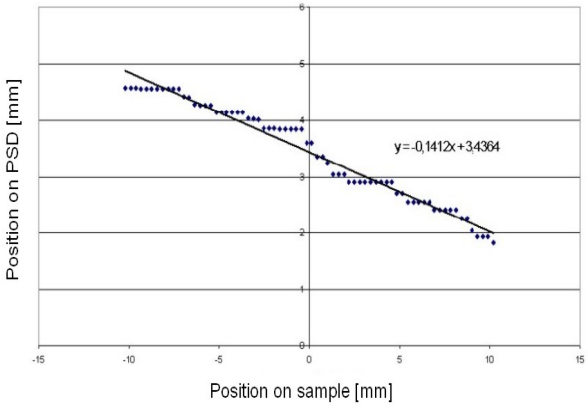


*Fig. 7. Deflection of the laser beam during the measurement.*

The biggest radius measurable, and therewith the smallest resolution for this set up is given by the noise of the PSD and the smallest quantization step of the A/D converter processing the PSD signal respectively. The current setup is capable of measuring radii up to 4km.

A more complex, though more sensitive setup [11, 12, 13] for measurement large radii up to 150km is shown in Fig. 8 and Fig 9.

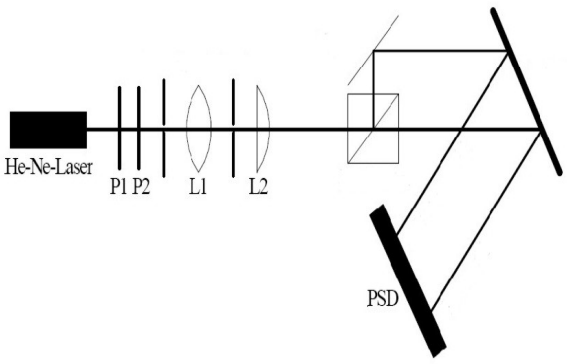


*Fig. 8. Setup to measure large curvatures P1, P2: polarization filters L1, L2: lenses to focus laser on PSD: „Position sensing diode".*

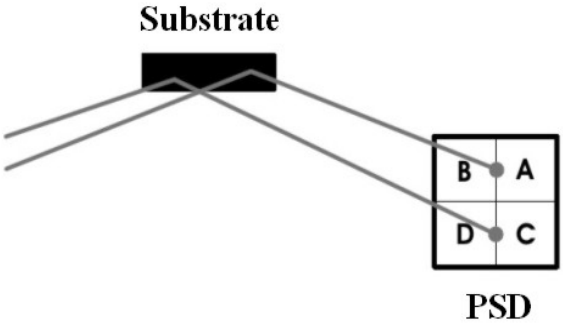


*Fig. 9. This setup utilizes a 4 quadrant detector.*

In this method a laser beam is splitted into two beams and a 4 quadrant detector is measuring directly the difference in the reflected angle of the two laser beams. By that

$$h''(x) = \frac{2}{R}x + b \tag{6}$$

is measured and the curvature thereby deduced in a very elegant way.

In both methods it is possible to lead the laser beam through a window into the deposition chamber to measure the formation of residual stress in situ.

Furthermore by using a heated substrate holder the temperature dependency of the residual stress can be measured and thereby information about the thermal expansion coefficients can be obtained which extends the value of the methods far over just measuring the residual stress [14].

## 5. Measurement of Residual stress in NCD

The films were deposited in a microwave plasma chemical vapour deposition process. A 2.45 GHz IPLAS CYRANNUS® plasma source was used [15]. As substrates (100) oriented silicon wafers with a thickness of 425µm were used. To enhance the nucleation of diamond the substrates were ultrasonically scratched for 30 min with a scratching solution consisting of diamond powder (~ 20 nm grain size), Ti powder (~ 5nm particle size) and Ethanol in a weight percent ratio of 1:1:100 (wt%). Afterwards the substrates were ultrasonically cleaned for 15 min in Acetone. During deposition the substrates were kept on a molybdenum substrate holder. Prior to the deposition the substrates were etched in a $H_2$/Ar plasma for 30 min. After this cleaning step the process parameters were switched to the deposition parameters.

The nanocrystalline diamond films shown in this work were deposited at a pressure of 200mbar in a Ar/$H_2$/$CH_4$ plasma for 5h. The methane fraction used in the process gas was 0.8% and the hydrogen fraction was varied between 2 % and 7 %. The amount of hydrogen was varied to investigate the influence of the hydrogen on the residual stress because it is known that hydrogen strongly affects the grain size in diamond growth [21] And because it was shown by the grain boundaries mismatch model that grain boundaries affect the residual stress, a strong influence of the hydrogen in the plasma on the stress is expected.

Fig. 10 shows scanning electron microscope pictures from one of the deposited NCD films.

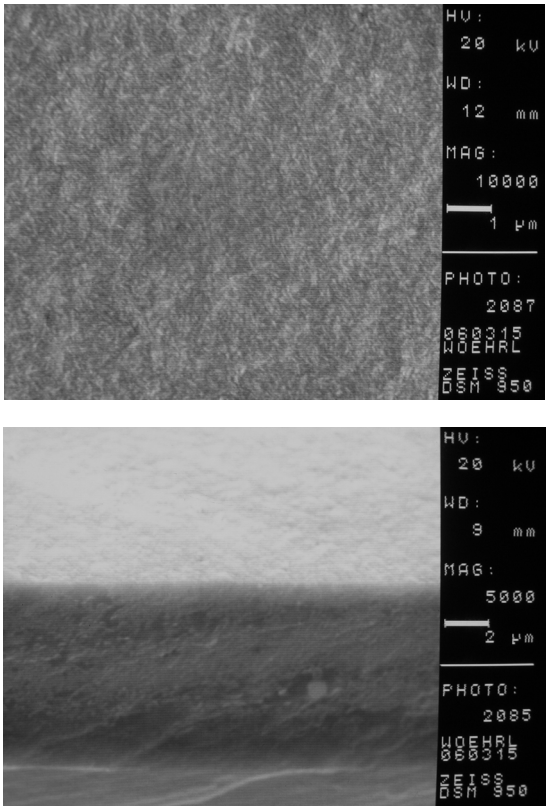


*Fig. 10. Top- and cross-sectional picture of an NCD film taken by scanning electron microscope (SEM).*

The film thicknesses of the deposited films are between 15µm and 30µm depending on the amount of hydrogen in the process gas.

For thick films the film bending moment and resultant flexure stress are no longer negligible and the film/substrate structure must be treated as a composite beam as Windischmann and coworkers worked out for diamond films [16].

Because the film thickness investigated in this work is relatively large the Brenner-Senderoff equation must be used to avoid substantial errors in the calculated stress [17]

$$S = S_0\left(1 + 4R\frac{t_{film}}{t_{Sub}} - \frac{t_{film}}{t_{Sub}}\right) \tag{7}$$

where R is the ratio of the film and substrate biaxial moduli (6.08 for polycrystalline diamond on (100) silicon) and $S_0$ is the stress derived from the Stoney equation.

Fig. 11 shows the results for the residual stress measurements obtained with respect to Stoney equation and the Brenner-Senderoff equation.

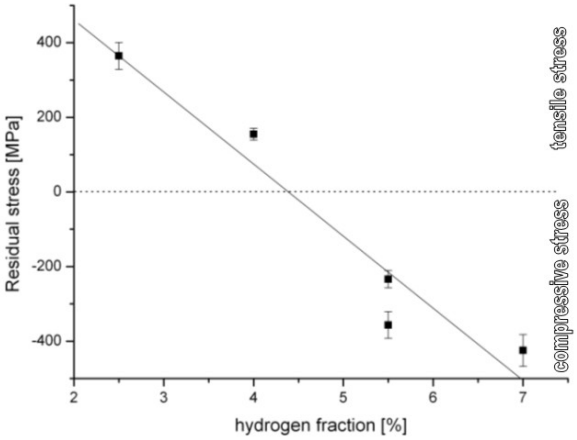


*Fig. 11 Residual Stress in NCD films.*

The residual stress is plotted versus the hydrogen fraction in the process gas. Both tensile and compressive stresses are measured. Per definition compressive stress is negative and tensile stress is positive.

It is shown that for small amounts of hydrogen tensile stress is measured in the films. This is different as soon as the hydrogen fraction is increased over 4.5%. Beyond this amount compressive stress is measured. This finding is greatly interesting, firstly because it is possible to adjust the residual stress in NCD films in a wide range just by changing the amount of hydrogen in the process gas, and secondly because it is thereby possible to find process parameter where stress free NCD films can be deposited.

As mentioned before, the residual stress consists of the two components thermal stress and intrinsic stress. If one wants to understand the influence of hydrogen one the residual stress the two components of the residual stress must be examined separately. The thermal stress can be calculated relatively simple with respect to equation 2. However in this equation only the mean values for the thermal expansion coefficients are used, which can lead to substantial errors in the case of high deposition temperatures and thermal expansion coefficients that change strongly with temperature.

In Fig. 12 the temperature dependence of the thermal expansion coefficient of silicon and diamond is shown. The thermal component of the residual stress can now be calculated by taking the integral of the thermal expansion coefficient over the temperature and one gets the curvature of the sample that arouse from the thermal stress [17] accordant to equation 5.

$$\frac{1}{R} = \frac{6(1+m)^2 \int_{T_r}^{T_d} (\alpha_s - \alpha_f)dt}{h\left[3(1+m)^2 + (1+mn)\left(m^2 + \frac{1}{mn}\right)\right]} \qquad (8)$$

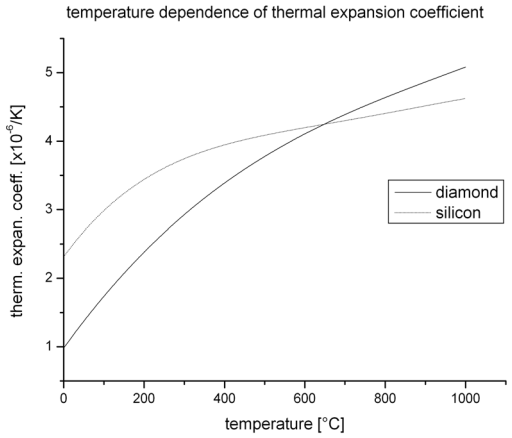


*Fig. 12. Thermal expansion coefficient of diamond and silicon.*

By subtracting the thermal stress from the measured residual stress one can deduce the intrinsic stress in the films as shown in Fig. 13 for the NCD films.

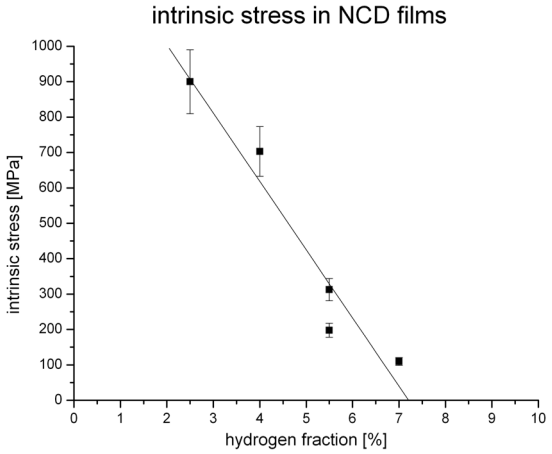


*Fig. 13. Intrinsic stress in the NCD films.*

Thus the residual stress in the NCD films consists of a compressive thermal component and an intrinsic component that is tensile for all the deposited films. The results suggest that the intrinsic tensile stress can strongly be influenced by the hydrogen admixture in the process gas. For low amounts of hydrogen the tensile stress in the film is rather high at around 1000 MPa. By adding more hydrogen to the process gas the films are less tensile stressed. At a concentration of 7 % of hydrogen the tensile stress is as low as 100 MPa in the film.

As mentioned above the tensile stress usually results from the grain boundaries (grain boundary mismatch model). Extending this model to 3D-nanostructured materials like NCD – here diamond grains in an amorphous matrix – one can look at grain boundries as amorphous material; but in NCD the thickness or amount

ot of this amorphous matrix can be systematically varied. Adding hydrogen to the process gas leads to larger diamond crystals in the film [9] and therefore the amount of this matrix (former grain boundaries density) is decreased as can be explained by a simple model: A given film volume is filled with idealized cubic crystals of equal edge length $a$. The volume of the film $V_f$ is than filled with $N$ crystals of the Volume $a^3$.

$$V_f = N \cdot a^3 \Rightarrow N = \frac{V_f}{a^3} \tag{9}$$

The surface area of the crystals is given by the six sides of the crystal cubes in this model and the area of one side given by $a^2$. Because every crystal is directly neighboured by another crystal every side wall is the side wall of two crystals, the overall surface area $A_f$ is therefore given by:

$$A_f = 3 \cdot N \cdot a^2 \tag{10}$$

Using equation 9 and equation 10 one can eliminate the actual number of crystals and calculate the surface area by:

$$A_f = 3 \cdot V_f \cdot \frac{1}{a} \tag{11}$$

Using the thickness of the matrix between the grains ("grain boundaries") $d$ one can now calculate the overall volume of this contribution by

$$V_g = d \cdot A_f = 3 \cdot V_f \cdot \frac{d}{a} \tag{12}$$

Anyway even for more realistic shapes there will be

$$\frac{V_g}{V_f} \sim \frac{d}{a} \tag{13}$$

The density of the grain size is because of its disordered structure lower than the density of the diamond crystals and therefore the expression $V_g/V_f$ equals the density change in the film. Intrinsic stress directly results from films being under- or overdense (giving tensile or compressive stress respectively); the relation between intrinsic stress and density in this case is thus given with respect to equation 13 by

$$\frac{\Delta\rho}{\rho} \sim \frac{V_g}{V_f} \sim \sigma \sim \frac{1}{a} \tag{14}$$

By reducing the hydrogen in the process gas one is decreasing the grain size of the diamond grains and thus increasing the amount of the matrix and according to equation 14 the tensile stress becomes lower as shown in Fig. 13.

With the assumption that the thickness of the matrix is not significantly changing – as in the original grain boundaries mismatch model - one can see that the volume of the grain boundaries normalized to the volume of the film is inverse proportional to the grain size. The relation given by equation 14 between the grain size and the tensile stress in films is then again consistent with thegrain boundaries mismatch model given by Hoffmann [5].

Since the intrinsic stress thus correlates with the volume of the grain boundaries it would be desirable to measure this part directly e.g. with spectroscopic methods. This would make it possible to perform non-destructive measurements of the intrinsic stress in any given sample independent of size and shape of the specimen. The applicability for routinely determination of stress in workpieces and thereby for the quality control could be expanded.

An ideal tool provides Raman Spectroscopy. For years Raman Spectroscopy is now used for characterization of carbon films [19]. A specific characteristic of visible light Raman Spectroscopy of carbon films is the small cross section of $sp^3$ bonded carbon compared to that of $sp^2$ bonded carbon [20]. This is the reason why Raman Spectroscopy, in the case of investigating NCD films, nearly exclusively provides information from the matrix and virtually no information from the $sp^3$ bonded carbon in the nanocrystalline diamond grains. Thus Raman

Spectroscopy gives a direct finger print of the matrix although the majority of the carbon atoms are actually $sp^3$ bonded carbon in the diamond grains [21].

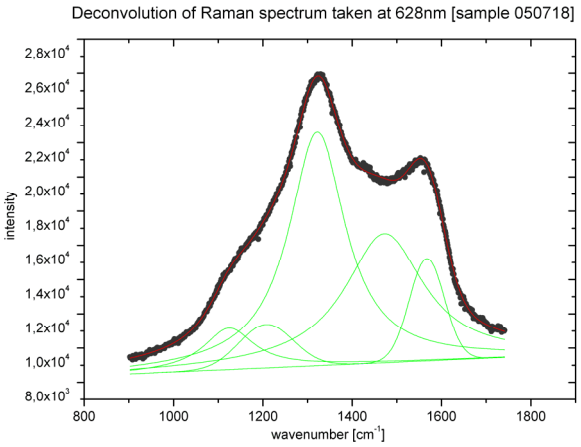


*Fig. 14. Raman spectrum of a NCD film.*

Fig. 14 shows a Raman spectrum (investigated with a HeNe laser with a wavelength of λ=632.8 nm) of a NCD film that was deposited with a hydrogen fraction of 2.5% in the process gas. The spectrum was deconvoluted and shows the characteristic features of amorphous carbon films with the D-Peak ("disordered") at around 1350cm$^{-1}$ and the G-Peak ("graphitic") at around 1580cm$^{-1}$. In

addition to these two peaks the spectrum features other characteristics that are assigned to nanocrystalline diamond in the literature, such as the peaks at around 1150cm$^{-1}$ and 1480cm$^{-1}$.

The Raman spectra of the NCD films were investigated to find a correlation with the intrinsic stress in the films, especially with the peaks around 1150cm$^{-1}$ und 1480cm$^{-1}$, whose origin is supposed to be in the amorphous matrix. The intensity of these grain boundaries related signals should be proportional to the volume of the grain boundaries and therewith proportional to the intrinsic tensile stress.

Intensities in Raman Spectroscopy are only comparable when normalized to other spectral features, to eliminate experimental variations, e.g. a variation in the laser power. Although there is no such feature which is inherently independent of the hydrogen in the process gas, the normalization of the 1150cm$^{-1}$ and the 1480cm$^{-1}$ peaks with the D- and the G-Peak gives a clear trend, which is shown in Fig. 15: The intensity of the peaks is proportional to the intrinsic stress measured by SSIOD. The intensity rises by a factor of three for the films under high tensile stress (around 1000 MPa) compared to the relatively stress-free films (100 MPa).

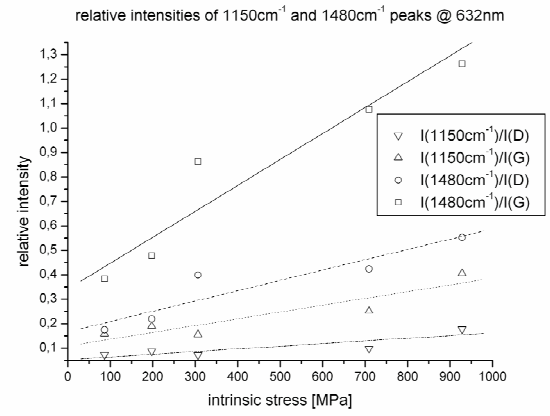


*Fig. 15. Rrelative intensities of the Raman peaks in correlation to the intrinsic stress in the films.*

## 6. Conclusion

The understanding of the origin of the residual stress in nanocrystalline diamond films is an important aspect when it comes to establishing NCD as a serious material for thin film technology. It was shown for NCD films how information regarding the thermal stress and the intrinsic stress were worked out from these measurements. Additionally it was shown that it is possible to deposit stress-free films when process parameters are chosen right.

The understanding of these fundamental phenomena leads to anew possibility for the non-destructive measurement of intrinsic stress in nanocrystalline diamond films. While up to now it was necessary to use special methods to measure the residual stress literally “in the laboratory” on flat substrates coated additionally beneath the workpiece, it is now possible to characterize coated work pieces directly from the production regarding to their intrinsic stress.

The key to this novel method is the quantitatively determination of the volume ratio of the grains and the amorphous matrix and their correlation with the intrinsic stress, because the measurement can be performed by spectroscopic methods – preferable Raman spectroscopy.

## References

[1] X. Xiao, J. Birrell, J. E. Gerbi, O. Auciello, J. A. Carlisle, J. Appl. Phys. **96**(4), 2232 (2004).
[2] G. G. Stoney, Proc. R. Soc. Lond. Ser. A **82**, 172, (1909)
[3] H. Windischmann, G. F. Epps, Y. Cong, R. W. Collins, J. Appl. Phys. **69**(4), 2231 (1991)
[4] N. Woehrl, V. Buck; Verhandl. DPG (VI) 41, DS 7.7, (2006), (in german)
[5] R. W. Hoffman, Thin Solid Films **34**, 185 (1976).
[6] H. Windischmann, Journal of Applied Physics **62**, 1800 (1987).
[7] V. Buck, Z. Physik B **33**, 349 (1979).
[8] V. Buck, 7th Intern. Conf. Ion & Plasma Assisted Techniques 267, (1989)
[9] M. Moske, K. Samwer, Rev. Sci. Instrum. **59**(9), 2012, (1988)
[10] J. T. Pan, I. Blech, J. Appl. Phys. **55**, 2874 (1984).
[11] H. Ibach, Surf. Sci. Rep. **29**, 193 (1997).
[12] D. Sander J. Phys.: Condens. Matter **16**, R603 (2004)
[13] P. Kury, T. Grabosch, M. Horn- von Hoegen, Rev. Sci. Instrum. 76, (2005).
[14] N. Woehrl, T. Hirte, V. Buck, Diam. Relat. Mater., to be published.
[15] CYRANNUS® I: European Patent No. 0, 872 164, USA Patent No. 6, 198, 224.
[16] H. Windischmann, K.J. Gray, Diam. Relat. Mater. **4**, 837 (1995).
[17] A. Brenner, S. Senderhoff, J. Res. Nat. Bur. Stand., **42**, 105 (1949).
[18] Q. H. Fan, J. Grácio, E. Pereira, J. Appl. Phys. **87**, 2880 (2000)
[19] A. C. Ferrari, J. Robertson, Phil. Trans. R. Soc. Lond. A **362**, 2477 (2004)
[20] N. Wada, P. J. Gaczi, A. Solin, J. Non-cryst. Solids **35-36**, 543 (1980)
[21] J. Birrell, J.E. Gerbi, O. Auciello, J.M. Gibson, J. Johnson, J.A. Carlisle, Diam. Relat. Mater. **14**, 86 (2005).

*Corresponding author: nicolas.woehrl@uni-due.de